THERMOMECHANICAL COUPLING EFFECTS ON LOW-CYCLE FATIGUE LIFE OF METALLIC MATERIALS

Pedro Manuel Calas Lopes Pacheco
Mechanical Engineering Department - CEFET/RJ, Av. Maracanã 229, Maracanã - 20271-110, Rio de Janeiro, RJ – Brazil
calas@cefet-rj.br

Heraldo da Costa-Mattos
Laboratório de Mecânica Teórica e Aplicada, Departamento de Engenharia Mecânica, Universidade Federal Fluminense
Rua Passo da Pátria 156, 24210-240, Niterói, RJ, Brasil
heraldo@mec.uff.br

Abstract. *The hypothesis of isothermal processes is often used to predict low-cycle fatigue life of structural elements. For high inelastic amplitudes and/or high frequencies, a considerable amount of heat can be generated, promoting the material softening and a decrease in the lifetime. In this paper, a anisothermal model based on the framework of continuum damage mechanics is proposed to study the thermomechanical coupling effects on low-cycle fatigue life of metallic materials. Simple numerical simulations of 316L stainless steel bars are presented and analyzed showing that the hypothesis of isothermal processes may be inadequate when cyclic inelastic deformations are involved. The results show that part of plastic work is transformed into heat, resulting in a temperature rise that affects substantially the mechanical behavior of the material.*

Keywords*: Low-Cycle Fatigue, Thermomechanical Coupling, Damage Mechanics, Modeling.*

1- Introduction

Inelastic cyclic deformation promotes heating of metallic structural elements. For high loading rates and/or high amplitudes of inelastic deformation, a considerable amount of heat can be generated (Simo, Miehe, 1992; Pacheco, 1994; Barbosa, Pacheco, Costa-Mattos, 1995). The temperature increasing in a mechanical component depends on loading amplitude, frequency and temperature boundary conditions. However, in traditional low-cycle fatigue models, the variation of the material temperature due to thermomechanical coupling is not considered and unreal life predictions may be obtained. Indeed, there are situations where such coupling cannot be neglected and a physically realistic model must consider it.

Since temperature variation can interfere on the fatigue phenomena and most classical low-cycle fatigue models only take into account isothermal processes, the ASTM standard for low-cycle fatigue testing (ASTM, 1980) establishes that the gradient of temperature during the testing program must not exceed a range of $\pm$ 2 K. For high inelastic amplitudes the standard recommends the use of cooling devices and low loading frequencies to maintain the specimen temperature within the established range. However, this is a difficult condition to achieve in real mechanical components in operation.

In this paper, a continuum damage mechanics model is proposed to study the thermomechanical coupling effects on the life prediction of metallic structures submitted to cyclic inelastic loadings (Pacheco, 1994; Lemaitre, Chaboche, 1990). A thermodynamic approach permits a rational identification of the thermomechanical coupling in the mechanical and thermal equations.

Numerical simulations of austenitic stainless steel (AISI 316L) bars submitted to cyclic loadings are presented and analysed.

2- Elasto-viscoplastic Model

The model used in this paper was proposed by Pacheco (Pacheco, 1994) and is developed within the framework of the thermodynamics of the irreversible processes. Such model is a generalization of the elasto-viscoplastic model proposed by (ASTM, 1980) for isothermal processes. For the elasto-viscoplastic material, the thermodynamic state is completely determined by the so-called state observable variables: total deformation ($\underline{\underline{\varepsilon}}$) and absolute temperature (θ) and by a set of internal variables: plastic deformation ($\underline{\underline{\varepsilon}}^p$), isotropic hardening (p), kinematic hardening ($\underline{\underline{c}}$) and damage (D). The macroscopic quantity D ($0 \le D \le 1$) represents the material local degradation. When D = 0 the material is in a virgin state and when D = 1 the material is completely damaged.

The elasto-viscoplastic behavior is characterized by two thermodynamic potentials: the Helmholtz free energy (Ψ) and the potential of dissipation (ϕ). The Helmholtz free energy can be written in terms of deformation energy density (W):

$$\rho\,\psi(\underline{\underline{\varepsilon}},\underline{\underline{\varepsilon}}^p,\gamma,\theta) = W_e(\underline{\underline{\varepsilon}}-\underline{\underline{\varepsilon}}^p,\gamma,\theta) + W_a(\gamma,\theta) - W_\theta(\theta) \qquad (1)$$

where ρ is the density of the material. For isotropic thermoelasticity the elastic energy density is expressed as:

$$W_e(\underline{\underline{\varepsilon}}-\underline{\underline{\varepsilon}}^p,\theta)=\frac{E}{2(1+\nu)}\left[(\underline{\underline{\varepsilon}}-\underline{\underline{\varepsilon}}^p).(\underline{\underline{\varepsilon}}-\underline{\underline{\varepsilon}}^p)+\frac{\nu}{1-2\nu}\left(tr(\underline{\underline{\varepsilon}}-\underline{\underline{\varepsilon}}^p)\right)^2\right]- \\ -\frac{\alpha E}{1-2\nu}(\theta-\theta_0)\,tr(\underline{\underline{\varepsilon}}-\underline{\underline{\varepsilon}}^p) \tag{2}$$

The energy densities associated to the hardening and to the temperature are:

$$\begin{cases} W_a(p,\underline{\underline{c}}) = W_p(p) + W_c(\underline{\underline{c}}) \\ W_p(p) = b\left(p + (1/d)e^{-dp}\right) \\ W_c(\underline{\underline{c}}) = (1/2)\,a\,(\underline{\underline{c}}.\underline{\underline{c}}) \end{cases} \tag{3}$$

where E, ν, α, b, d and a are temperature-sensitive material parameters, C_1 and C_2 are positive constants and θ_0 a reference temperature. To simplify the notation, a variable β is used to represent the set of internal variables (p,$\underline{\underline{c}}$,D).

The thermodynamic forces ($\underline{\underline{\sigma}}$,$B^\beta$,s), associated to the state variables ($\underline{\underline{\varepsilon}}$,β,θ), are defined from ψ, as follows:

$$\underline{\underline{\sigma}} = \rho\frac{\partial\psi}{\partial\underline{\underline{\varepsilon}}}\ ;\ B^\beta = -\rho\frac{\partial\psi}{\partial\beta}\ ;\ s=-\frac{\partial\psi}{\partial\theta} \tag{4}$$

The elasto-viscoplastic materials are characterised by a elastic domain in the stress space where yielding doesn't occur. There exists a yielding function: $F(\underline{\underline{\sigma}},B^\gamma,\underline{\underline{\varepsilon}}^p,\gamma,\theta)$, where $\dot{\underline{\underline{\varepsilon}}}^p = \underline{\underline{0}}$ and $\dot{\beta} = 0$, if $F(\underline{\underline{\sigma}},B^\beta;\underline{\underline{\varepsilon}}^p,\beta,\theta) < 0$. The yielding function has the form:

$$\begin{cases} F(\underline{\underline{\sigma}},B^p,\underline{\underline{B}}^c;\underline{\underline{c}},\theta)= f(\underline{\underline{\sigma}},B^p,\underline{\underline{B}}^c;\theta) +(\frac{\varphi}{2})\left[\left(\underline{\underline{B}}^c.\underline{\underline{B}}^c\right)-a^2(\underline{\underline{c}}.\underline{\underline{c}})\right] \\ f(\underline{\underline{\sigma}},B^p,\underline{\underline{B}}^c;\theta)= J(\underline{\underline{\sigma}}+\underline{\underline{B}}^c) +B^p\ -\sigma_p \\ J(\underline{\underline{\sigma}}+\underline{\underline{B}}^c)= \left[(3/2)(\underline{\underline{\sigma}}+\underline{\underline{B}}^c)_{dev}.(\underline{\underline{\sigma}}+\underline{\underline{B}}^c)_{dev}\right]^{1/2} \end{cases} \tag{5}$$

where σ_p is the limit of proportionality, φ a material parameter and $(\ )_{dev}$ represents the deviatoric part of a tensor.

The potential of dissipation can be separated in two parts: $\phi^*(\underline{\underline{\sigma}},B^\beta,\underline{g}) = \phi_1^*(\underline{\underline{\sigma}},B^\beta) + \phi_2^*(\underline{g})$, with

$$\begin{cases} \phi_1^* = \dfrac{k}{n+1}\left\langle\dfrac{F(\underline{\underline{\sigma}},B^\beta;\underline{\underline{\varepsilon}}^p,\beta,\theta)}{k}\right\rangle^{n+1} \\ \phi_2^* = (\theta/2)\,\Lambda\,[\underline{\underline{I}}\,\underline{g}].g \end{cases} \tag{6}$$

where $\underline{q}$ are the heat flux, $\underline{g} = \nabla\theta/\theta$ and k, n and Λ are material parameters that depends on the temperature.

A set of constitutive equations, called the evolution laws, which characterizes the evolution of the dissipative processes, are obtained from ϕ*:

$$\dot{\underline{\underline{\varepsilon}}}^p = \frac{\partial\phi^*}{\partial\underline{\underline{\sigma}}}\quad ;\quad \dot{\beta} = \frac{\partial\phi^*}{\partial B^\beta}\quad ;\quad \underline{q} = \frac{\partial\phi^*}{\partial\underline{g}} \tag{7}$$

Using the set of constitutive equations (2.4, 2.7), the heat equation can be written as (Pacheco, 1994):

$$div\left(\underline{\underline{\Lambda I}}\,\nabla\theta\right)-\rho c\dot{\theta}=-\underline{\underline{\sigma}}\,\dot{\underline{\underline{\varepsilon}}}^p - B^\beta\dot{\beta}+\theta\left(-\frac{\partial\underline{\underline{\sigma}}}{\partial\theta}.(\dot{\underline{\underline{\varepsilon}}}-\dot{\underline{\underline{\varepsilon}}}^p)+\frac{\partial B^\beta}{\partial\theta}\dot{\beta}\right) \tag{8}$$

The following local version of the second law of thermodynamics can be obtained:

$$\begin{cases} d_1 = \underline{\underline{\sigma}}.\dot{\underline{\underline{\varepsilon}}}^p + B^\beta \dot{\beta} \geq 0 \\ d_2 = -(\underline{q}.\underline{g}) \geq 0 \end{cases} \tag{9}$$

where d_1 represents the mechanical dissipation and d_2 the thermal dissipation. It can be shown that the set of constitutive equations formed by (4) and (7) will always verify the inequalities (9).

The term d_1 appears in the right hand side of the heat equation (8) and will be called internal coupling. It is always positive and has a role in (8) similar to a heat source in the classical heat equation for rigid bodies. The last term in the right hand side of the heat equation, can be positive or negative and will be called the thermal coupling:

$$\text{acpT} = \theta\left(\frac{\partial \underline{\underline{\sigma}}}{\partial\theta}:(\dot{\underline{\underline{\varepsilon}}}-\dot{\underline{\underline{\varepsilon}}}^p) - \frac{\partial B^\beta}{\partial\theta}\dot{\beta}\right) \tag{10}$$

In metal forming the thermomechanical coupling is usually taken into account by an empirical constant called the heat conversion factor (Simo, Miehe, 1992; Kobayashi, Oh, Altan, 1989). It represents the part of plastic power transformed into heat:

$$\chi = \frac{d_1 + \text{acpT}}{\underline{\underline{\sigma}}.\dot{\underline{\underline{\varepsilon}}}^p} \tag{11}$$

3- Elasto-viscoplastic Bars

Uniaxial bars immersed in a medium with constant temperature and subjected to prescribed axial displacement loadings are considered in this work. This simple geometry offers a good enlightenment in the analysis of the thermocoupling effects in fatigue life of metallic components and permits a direct comparison with experimental results obtained from specimens of traditional low-cycle fatigue testing. For the uniaxial case, the set of equations (2.4,2.7) can be reduced to (Lemaitre, Chaboche, 1990):

$$\begin{cases} \dot{\varepsilon}^p = (3/2)\left\langle \dfrac{|\sigma\text{-}X| - R - \sigma_P}{k} \right\rangle^n \dfrac{\sigma\text{-}X}{|\sigma\text{-}X|} \\ \dot{p} = |\dot{\varepsilon}^p| \\ \dot{c}_1 = \dot{\varepsilon}^p - (2/3)(\varphi_1/a_1)(1\text{-}D)X_1\dot{p} \;\; ; \;\; \dot{c}_2 = \dot{\varepsilon}^p - (2/3)(\varphi_2/a_2)(1\text{-}D)X_2\dot{p} \\ \dot{D} = \dfrac{B^D}{S_0}\,\dot{p} \\ \sigma = (1\text{-}D)E\left[(\varepsilon\text{-}\varepsilon^p) - \alpha(\theta\text{-}\theta_0)\right] \\ R = (1\text{-}D)\, b\left[1\text{-}e^{-dp}\right] \\ X = (3/2)\,(1\text{-}D)(a\,c) \;\; ; \;\; X = X_1 + X_2 \;\; ; \;\; c = c_1 + c_2 \end{cases} \tag{13}$$

When there is no internal source present and the traditional hypothesis adopted in the study of fins are considered, the heat equation (8) can be written as (x denotes the axial direction):

$$\frac{\partial}{\partial x}\left(\Lambda\frac{\partial\theta}{\partial x}\right) - \frac{hP}{A}(\theta\text{-}\theta_\infty) - \rho c\dot{\theta} = -\sigma\dot{\varepsilon}^p + R\dot{p} + X\dot{c} - B^D\dot{D} - \theta\left(\frac{\partial\sigma}{\partial\theta}(\dot{\varepsilon}\text{-}\dot{\varepsilon}^p) + \frac{\partial R}{\partial\theta}\dot{p} + \frac{2}{3}\frac{\partial X}{\partial\theta}\dot{c} - \frac{\partial B^D}{\partial\theta}\dot{D}\right) \tag{14}$$

where X and R are auxiliary variables, respectively related with the kinematic and isotropic hardening. For now on, the variables X and R will be simply called kinematic and isotropic hardening. B^D a variable associated with the damage evolution and θ_0 the initial temperature of the bar which is the same as the medium temperature θ_∞ . Two kinematic hardening variables (c_1 and c_2) are used to model the material behaviour (Lemaitre, Chaboche, 1990). In the following analysis a linear dependency on temperature is considered for the material parameters k, n, σp, φ_1, φ_2, a_1, a_2, S_0, E, α, b, d, Λ, ρ and c. The constants h, P e A are, respectively, the convection coefficient, the perimeter and the cross section of the bar. The right side of equation (14) contains the thermomechanical coupling terms.

In the analysis of problems with prescribed displacement (u) loadings, the equilibrium equation and the strain-displacement relation must also be considered:

$$\frac{\partial \sigma}{\partial x} = 0 \quad ; \quad \frac{\partial u}{\partial x} = \varepsilon = \frac{\sigma}{(1-D)E} + \varepsilon^{p} + \alpha(\theta - \theta_0) \tag{15}$$

with the following boundary conditions: $u(x=0) = 0$; $u(x=L) = u_L(t)$, where L is the bar length.

4 - Numerical simulations

To study the thermocoupling effects in fatigue life of metallic components, the following analysis consider round bars of AISI 316L stainless steel with diameter (D) of 5 mm and length (L) of 50 mm submitted to prescribed cyclic displacement loadings (triangular shape) as shown in Figure 2. The bar have an initial temperature of 293 K (θ_i) and is immersed in a medium with a constant temperature of 293 K (θ_∞). Table 1 shows the material parameters for two distinct temperatures (Lemaitre and Chaboche, 1990; Peckner and Bernstein, 1977). A linear dependence on temperature is adopted in the analysis.

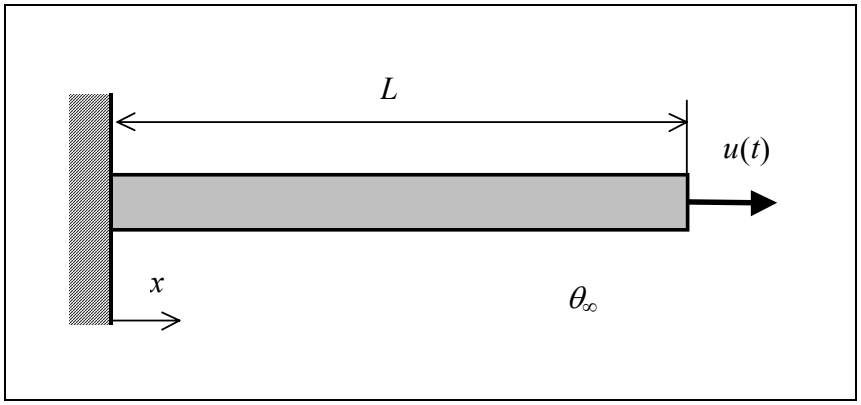

Figure 2 - Round bar submitted to a prescribed cyclic displacement loading.

Table 1 – Temperature Dependent Material Parameters (AISI 316L).

PARAMETER	VALUE	
	293 K (20°C)	873 K (600°C)
E (GPa)	196	150
σp (MPa)	82	6
k (MPa)	151	150
n (-)	24	12
b (MPa)	60	80
d (-)	8	10
a_1 (GPa)	108.3	17.5
φ_1 (-)	2800	350
a_2 (GPa)	4.5	1.0
φ_2 (-)	25	15
α (1x10^{-6}/K)	15.4	18.0
c (J/Kg K)	454	584
Λ (W/m K)	13	21

The coefficient S_0 presents a dependency with plastic deformation amplitude, and can be adequately represented by the following equation (Pacheco, 1994):

$$S_0 = k_f \, e^{-n_f \Delta \varepsilon^{p}} \tag{16}$$

where k_f and n_f are material parameters. For AISI 316L, k_f = 1.524 x 10^{11} Pa and n_f = 64.4 (Pacheco, 1994; Pacheco and Costa-Mattos, 1997).

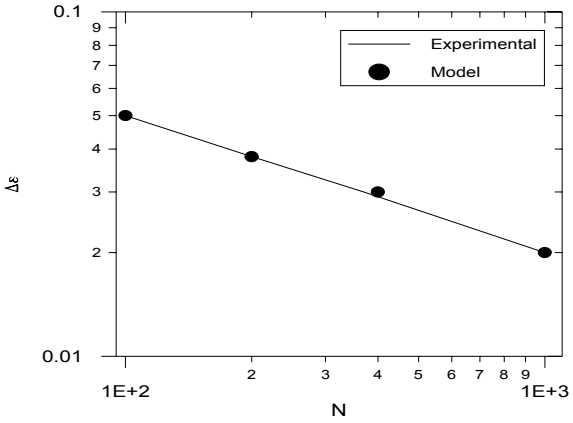

Figure 3 - ε x N curve for the stainless steel 316L (293 K) obtained with the *ASTM* recommendations for low-cycle fatigue test.

Figure 3 shows a comparison between experimental data from a low-cycle fatigue test (Bathias and Bailon, 1980) and model fatigue life prediction for the 316L stainless steel at room temperature. In the simulations, a combination of slow loadings rates and high convection coefficients is used (T = 100 s and h = 10 kW/m^2 K, where T is the loading period) to guarantee the temperature variation restriction of ± 2 K of the *ASTM* standard. This figure shows a good agreement between the experimental data and the predictions.

For ordinary mechanical components in operation this is a difficult condition to achieve and wrong predictions can be obtained if the thermomechanical coupling is not considered. As an example, consider a bar submitted to a prescribed displacement loading amplitude of ± 0.75 mm at one end (±1.5% mean strain) and with constant temperature boundary conditions at both ends. To study the influence of loading frequency and heat removal characteristics in the low-cycle fatigue life predictions, six thermomechanical loading conditions with different loading periods (T) and heat convection coefficients (h) are considered and are shown in Table 2. By symmetry considerations, only one half of the bar ($0 \le x \le L/2$) is studied with the following boundary conditions: at $x = 0$, $u = 0$ and $\theta = \theta_i$; at $x = L/2$, $u = u(t)$ – triangular loading with an amplitude of 0.375 mm – and $q = 0$. A convergence analysis is developed and a spatial discretization of 11 points with a time step corespondent to 400 point per cycle is adopted.

Table 2 – Thermomechanical Loading Conditions studied.

CONDITION	T (s)	h (W/m^2 K)
(1)	100	10,000
(2)	100	1,000
(3)	100	100
(4)	100	10
(5)	10	100
(6)	10	10

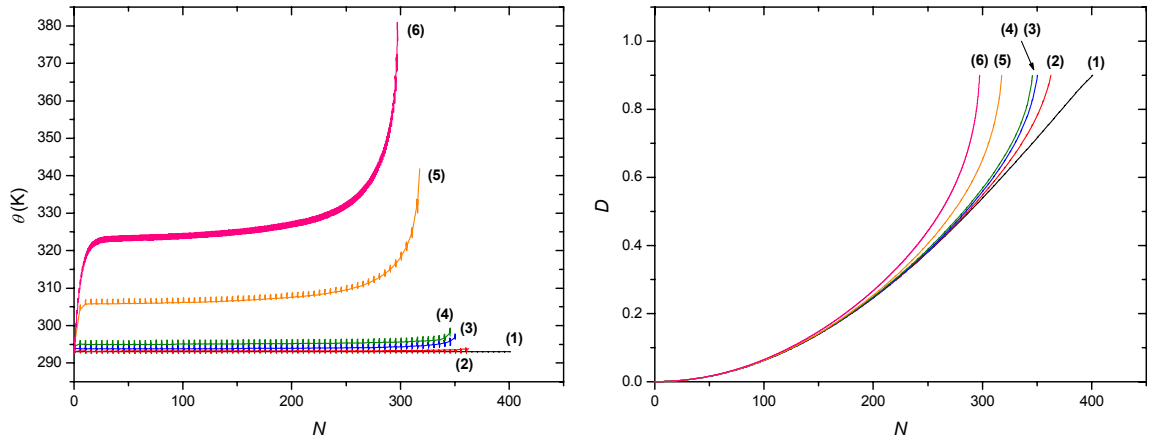

Figure 4 - Temperature (*a*) and damage (*b*) evolution at the bar midpoint for the six conditions considered.

Figure 4 shows temperature and damage evolution as a function of the number of loading cycles (N) at the bar midpoint ($x = L/2$) where a localization phenomenon is observed.

Situation **(1)** can be regarded as a testing of a specimen in compliance with the *ASTM* standard for low-cycle fatigue, where the variation of temperature does not exceed the ± 2 K range. In the other situations, this requirement is not obeyed and the temperature rise is enough to decrease the fatigue resistance of the material. A comparison between the six conditions is presented in Table 3. Also a relative variation in percent calculated considering the condition **(1)** as reference is shown in the table.

Conditions **(5)** and **(6)** presents a decrease in the life prediction of the bar of about one-quarter and a temperature rise of 52 and 84 K, respectively, which indicates a strong influence of the loading frequency in the amount of heat generated and, as a consequence, in the life of the bar.

The thermomechanical coupling can be seen as a feedback phenomenon. The heat generated by the mechanical process causes an increase of temperature, which promotes a decrease in the mechanical strength. Therefore, the plastic strain amplitude tends to increase causing a greater temperature rise and so on. Also it is important to observe that the temperature boundary conditions can lead to a localization process which can accelerate the feedback phenomenon.

In the following analysis, condition **(6)**, which presents the more dramatic life prediction reduction, is explored in more detail. Figure 5 shows the mechanical variables (stress, plastic strain, kinematic and isotropic hardenings) evolution at the bar midpoint ($x = L/2$).

Table 3 – Fatigue Life Prediction for Different Thermomechanical Loading Conditions.

CONDITION	N (cycles)	Δ (%)
(1)	401	-
(2)	363	-10
(3)	351	-13
(4)	346	-14
(5)	318	-21
(6)	297	-26

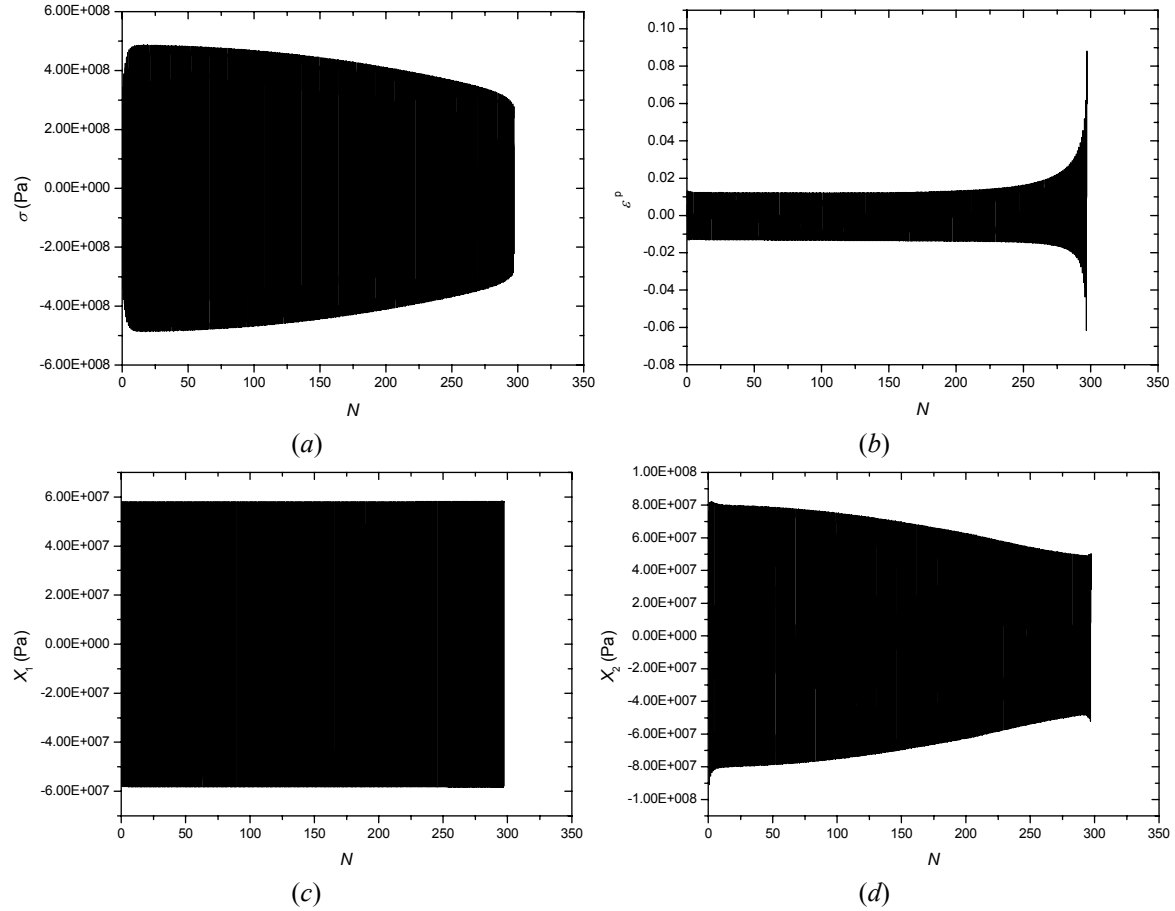

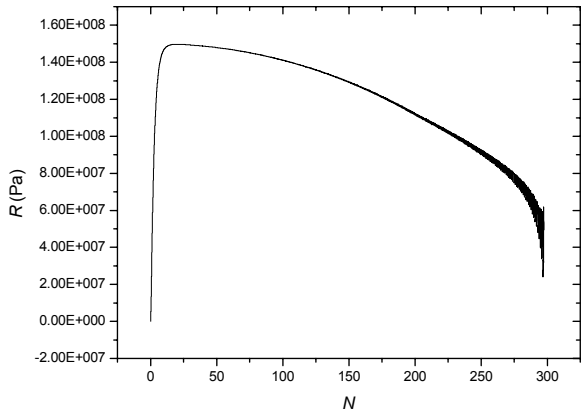

(*e*)

Figure 5 - Stress (*a*), plastic strain (*b*), kinematic hardening X (*c*-*d*) and isotropic hardening R (*e*) evolution at bar midpoint for condition (**6**).

Figure 6 shows the localization of the temperature, damage and accumulated plastic strain at the bar midpoint. Figure 7 shows the distribution of these three variables. For a better visualization, the distribution of the variables is shown through the whole bar.

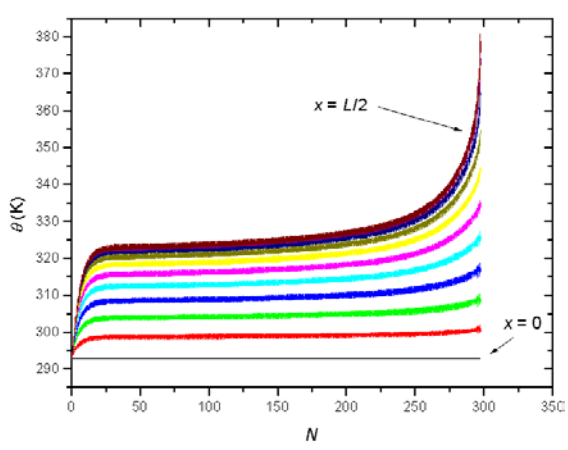

(*a*)

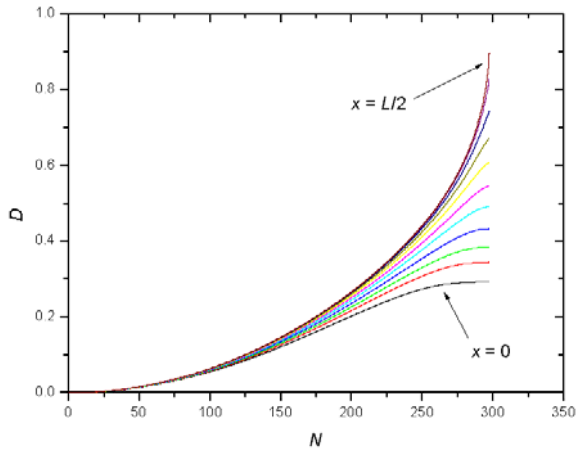

(*b*)

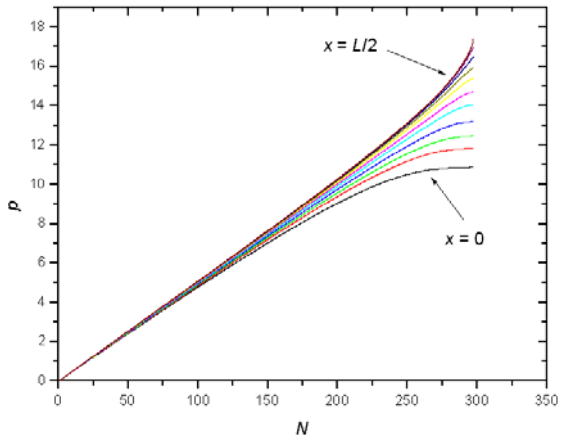

(*c*)

Figure 6 - Temperature (*a*), damage (*b*) and accumulated plastic strain (*c*) evolution at different points for condition **(6)**.

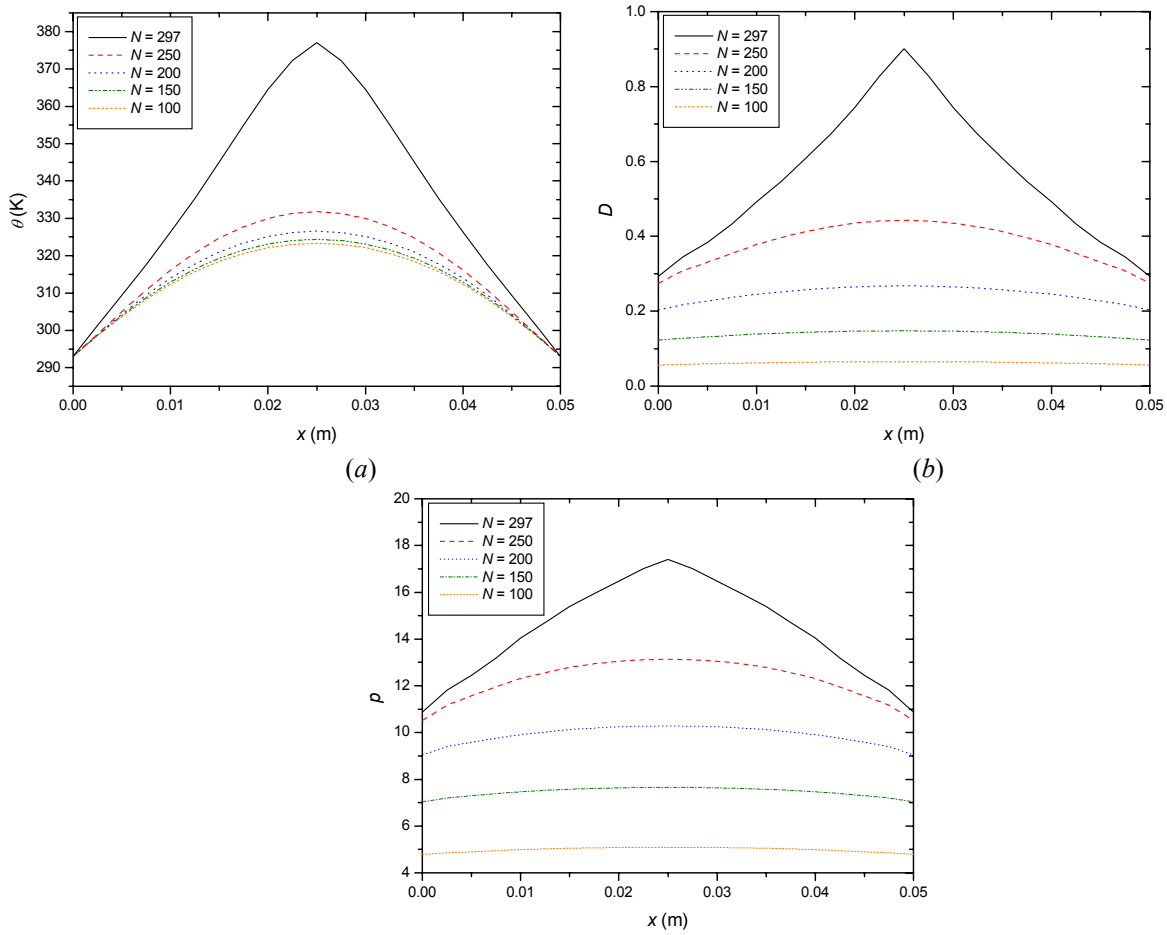

Figure 7 - Temperature (*a*), damage (*b*) and accumulated plastic strain (*c*) distribution for condition **(6)**.

At this point, the thermomechanical coupling terms are analyzed. Figure 8*a* shows the evolution of the internal coupling (d_1) and Figure 8*b* shows the evolution of the thermal coupling (*acpT*) at the bar midpoint. It is important to note that the second law of thermodynamics is not violated since the sum d = (d_1 + *acpT*) is always positive. At the bar midpoint, d_2 is always zero as a consequence of the adiabatic boundary condition and from Figure 8*a* d_1, which is equal to the internal coupling, is always greater than or equal to zero.

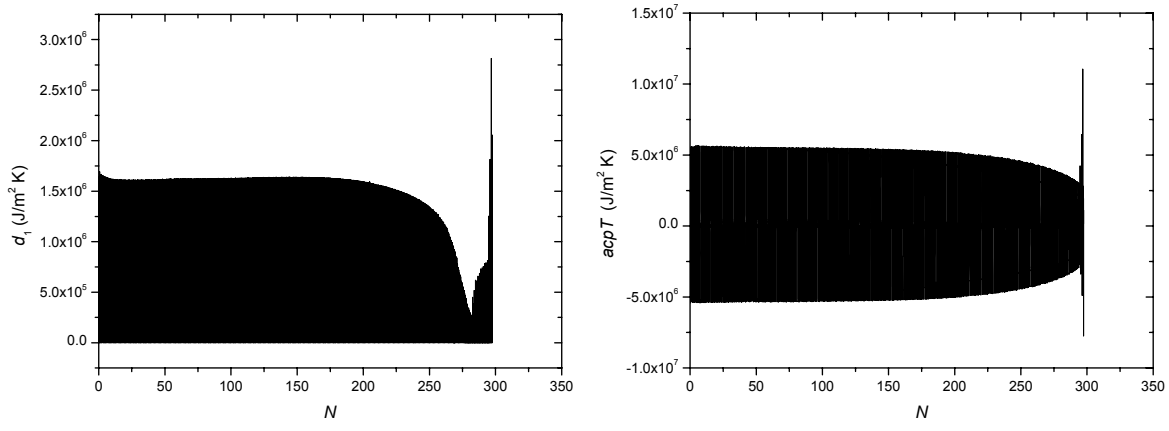

Figure 8 - Internal coupling (d_1) (*a*) and thermal coupling (*acpT*) (*b*) evolution at the bar midpoint for condition (**6**).

Figure 9 shows the evolution of each term of the internal coupling while Figure 10 shows the evolution of each term of the thermal coupling. A comparison between Figure 8 and Figures 9 and 10 reveals that for the internal coupling the term associated with plastic strain is predominant and for the thermal coupling the term associated with elastic strain is predominant.

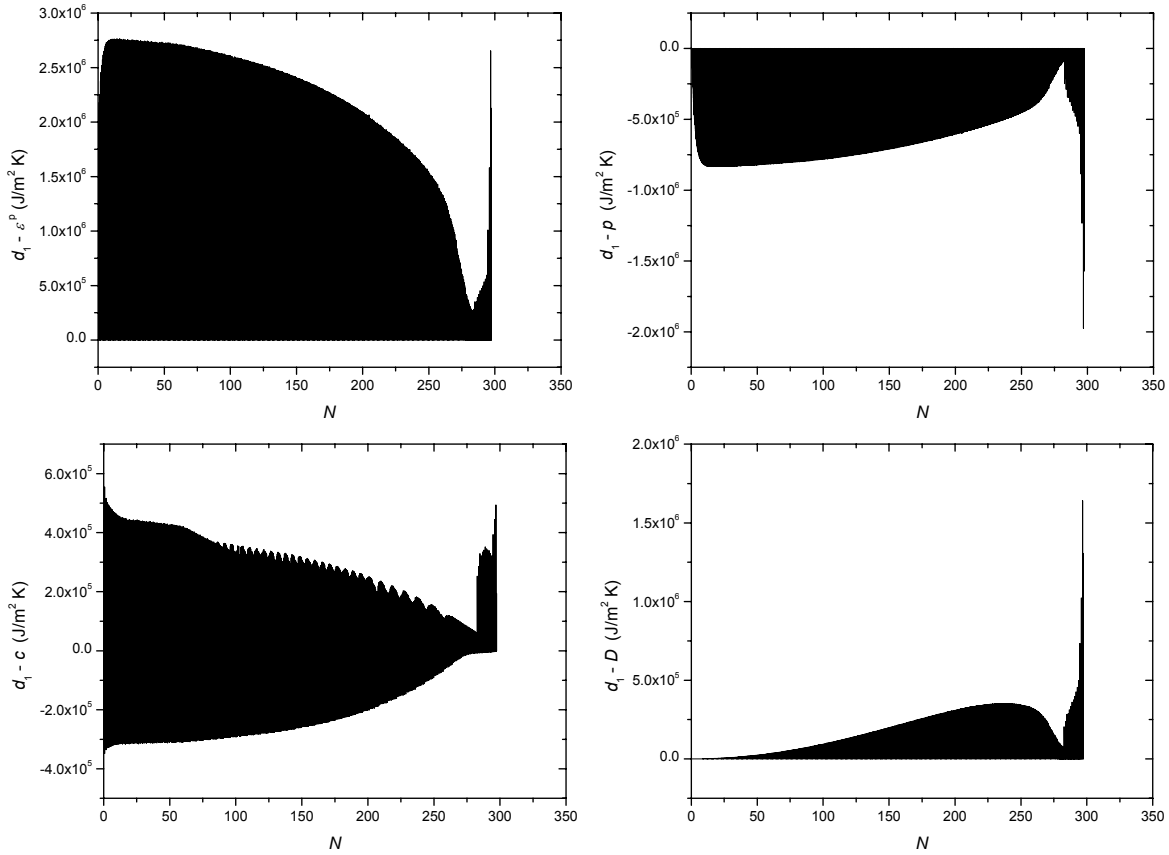

Figure 9 - Internal coupling terms evolution at the bar midpoint for condition (**6**).

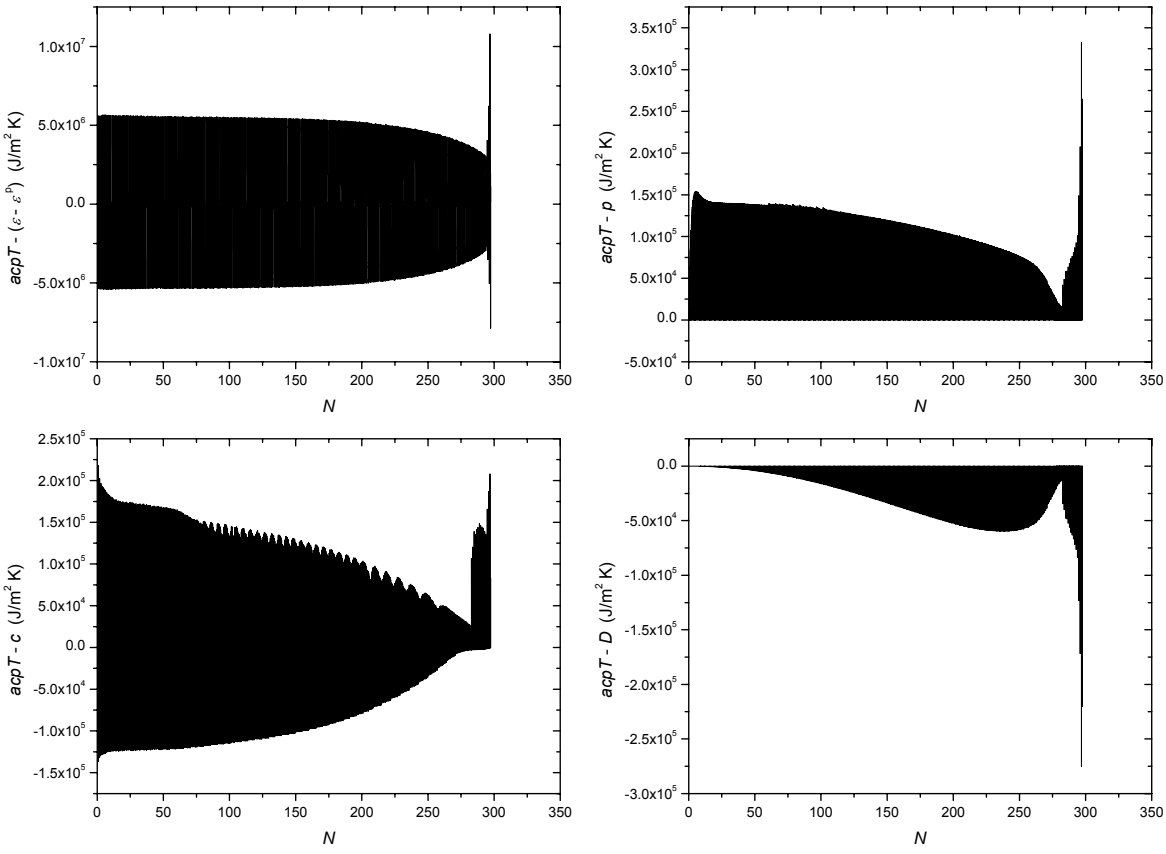

Figure 10 - Thermal coupling terms evolution at the bar midpoint for condition (**6**).

It is worth to note that the mechanic behavior strongly depends on the temperature distribution. Other mechanical and thermal conditions lead to different predictions. For example, adiabatic temperature boundary conditions at both ends lead to a homogeneous temperature distribution and different life predictions are observed for the six defined conditions. In this case a reduction of 3% and 6% is predicted for conditions **(4)** and **(6)**, respectively. In real life structures and mechanical components, thermal boundary conditions between adiabatic and constant temperature can be expected. In tensile tests, the perturbation in the temperature field caused by the end connections geometry is sufficient to strongly localize deformation in the middle of the bar, even if adiabatic conditions are considered.

5 - Conclusion

In this paper, an internal variable theory was proposed to study the thermomechanical coupling effects in elasto-viscoplastic bars subjected to mechanical loadings. This formulation provides a rational methodology to study complex phenomena like the amount of heat generated during plastic deformation of metals.

The numerical simulations show that it is important to consider the thermomechanical coupling effects in low-cycle fatigue projects of mechanical components, particularly when high loading rates are involved. In these situations, if the thermomechanical effect is not included in the model, wrong predictions can be obtained and unexpected failures may occur.

6 - References

ASTM E606-80, 1980, *Standard Recommended Practice for Constant-Amplitude Low-Cycle Fatigue Testing*, ASTM Standards, Vol. 03.01, 629-641.

Barbosa J.M.A., Pacheco P.M.C.L., Costa-Mattos H. S., 1995, On the role of Temperature in the Mechanical Vibration of Elasto-Viscoplastic Bars, *COBEM-95/CIDIM-95, XIII Brazilian Congress of Mechanical Engineering*, Belo Horizonte, Brazil, (in portuguese).

Barbosa, J.M.A., Pacheco, P.M.C.L. e Costa Mattos, H., 1997, "Rol de la Temperatura en las Vibraciones Mecanicas de Barras Elasto-viscoplasticas", *Revista Internacional de Información Tecnológica*, ISSN 0716-8756, Vol.8, No.6, pp.59-63.

Bathias C., Bailon J.P., 1980, *La Fatigue de Materiaux et des Structures*, Les Presses de L'Université de Montréal, Maloine S.A. Editeur, Paris.

Kobayashi S., Oh S., Altan T., 1989, *Metals Forming and the Finite Element Method*, Oxford Univ. Press.

Lemaitre J., Chaboche J.L., 1990, *Mechanics of Solids Materials*, Cambridge Univ. Press

Pacheco P.M.C.L., 1994, *Analysis of the Thermomechanical Coupling in Elasto- Viscoplastic Materials*, Ph.D.Thesis, Department of Mechanical Engineering, PUC-Rio (in Portuguese).

Pacheco, P.M.C.L. and Costa-Mattos, H. S., 1997, "Modeling the Thermomechanical Coupling Effects on Low-Cycle Fatigue of Metallic Materials", *5th ICBMFF, 5th International Conference on Biaxial/Multiaxial Fatigue and Fracture*, pp.291-301, Cracow, Poland.

.

Peckner, Bernstein, 1977, *Handbook of Stainless Steels*, McGraw-Hill.

Simo J.C., Miehe C., 1992, On the Coupled Thermomechanical Treatment of Necking Problems via Finite Element Methods, *Journal of Applied Methods in Engineering*, **33**, 869-883.

7. Responsibility notice

The author(s) is (are) the only responsible for the printed material included in this paper.